



HHS Public Access

Author manuscript

ACS Macro Lett. Author manuscript; available in PMC 2017 May 17.

Published in final edited form as:

ACS Macro Lett. 2016 May 17; 5(5): 636–640. doi:10.1021/acsmacrolett.6b00219.

Depolymerizable Poly(O-vinyl carbamate-*alt*-sulfones) as Customizable Macromolecular Scaffolds for Mucosal Drug Delivery

Kaushlendra Kumar, Eduard Jimenez Castaño, Andrew R. Weidner, Adem Yildirim, and Andrew P. Goodwin*

Department of Chemical and Biological Engineering, University of Colorado Boulder, Boulder, CO 80303, USA

Abstract

Interest in stimulus responsive materials and polymers has grown over the years, having shown great promise in a diverse set of applications. For drug delivery, stimulus-responsive polymers have been shown to encapsulate therapeutic cargo such as small molecule drugs or proteins, deliver them to specific locations in the body, and release them so that they can induce a therapeutic effect in the patient. Most hydrolytically degradable polymers are synthesized via nucleophilic, anionic, or cationic polymerization, which generally requires protection of nucleophilic or protic side chains prior to polymerization. Here, we report the synthesis of novel, alternating copolymers of sulfur dioxide and O-vinyl carbamate monomers that boast excellent functional group tolerance and pH-dependent instability. Alternating copolymers were synthesized containing pendant functionalities such as alcohol, carboxylic acid, ester, and azide without deprotection or post-polymerization modification. The copolymers were then formulated via nanoprecipitation into polymer nanoparticles capable of encapsulating small molecule dyes. The polymer nanoparticles were found to degrade rapidly at pH > 6 and were stable even in highly acidic conditions. Based on this observation, a proof-of-concept study for mucosal delivery was performed in polymer nanoparticles entrapped in a mucus model. At pH 8 the diffusion of encapsulated dye was found to be similar to free dye, while at pH 5 the diffusion coefficient was an order of magnitude lower. Cell viability was retained at 200 µg/mL particles after 24 h incubation. These polymers thus show promise as highly customizable scaffolds for mucosal drug delivery.

New polymer scaffolds are consistently being sought for drug delivery to improve drug bioavailability at diseased parts of the body while reducing off-target toxicity to healthy tissue. While encapsulation of drugs in polymer scaffolds can help to bias accumulation towards diseased tissue, methods must be developed to release the drug once it has reached a

*Corresponding Author. andrew.goodwin@colorado.edu.

ASSOCIATED CONTENT

Supporting Information. Characterization of monomers and polymers, ¹H NMR spectra, dye release vs. KO₂ concentration, Rhodamine B calibration curve for determining dye loading, and experimental methods. This material is available free of charge via the Internet at <http://pubs.acs.org>.

Author Contributions

The manuscript was written through contributions of all authors.

desired location. Thus, significant effort has been devoted to inducing chemical responses in polymer scaffolds based on changes in pH,¹ reducing environments,² enzymes,³ and light.^{4–5} Such stimuli-responsive polymer scaffolds have also been designed to amplify their response to stimuli to induce depolymerization, or breakdown of polymers into small molecule components.^{6–10} In order for such amplification to be effective, the polymer must remain stable upon administration but rapidly degrade into many small, easily-excreted molecules once the scaffold reaches its target destination, causing the concomitant release of any contents encapsulated within the polymer network.

In this work, we report a new type of depolymerizable scaffold that can be synthesized with excellent functional group tolerance via free radical polymerization. Free radical polymerization of vinyl-containing monomers results in a carbon chain that is stable to water, preventing breakdown in the body and eventual excretion. Instead, most depolymerizable macromolecules are synthesized via condensation polymerization, which results in the formation of polymers with repeating functional groups with hydrolytic instability, including poly(carbamates),⁷ poly(lactic-co-glycolic acid),^{11,12} poly(caprolactone),¹³ poly(carbonates),^{14,15} and poly(acetals).^{16–19} While these polymers have shown success in many stimulus-responsive drug delivery applications, they must be synthesized via nucleophilic, cationic, or anionic polymerization, which limits the scope of unprotected functional groups that can be incorporated to the polymerization procedure. As a result, adding synthetic complexity to these macromolecules may require additional stepwise modification to any resultant nanoparticles after their formulation.

We report here a novel class of aqueous depolymerizable macromolecules, poly(O-vinyl carbamate-*alt*-sulfones), that can be synthesized from free radical polymerization with excellent functional group tolerance. Sulfur dioxide has been shown to copolymerize with certain vinyl monomers in a specifically alternating manner, provided that the vinyl group is immediately adjacent to an electron-donating group; examples include vinyl acetate,²⁰ vinyl carbonate,^{20,21} and olefins.^{22–25} Such copolymers were originally developed as photoresists with sensitivity to deep UV and soft x-ray, but in more recent years they have been explored as thermally-sensitive materials for packaging.^{20–22} Both Moore and coworkers and Swager and coworkers have demonstrated that thermal decomposition properties can be tuned via changes in the alkyl monomer structure.^{20–22} Recently, our group showed that one such polymer, poly(vinyl acetate-*alt*-sulfur dioxide), degraded into its monomer components in the presence of biomedically relevant stimuli, such as reactive oxygen species and ultrasound.²⁶ However, a new monomer choice was required because vinyl esters with a customizable R group can be difficult to synthesize, as most syntheses of vinyl esters require transition metal catalyzed oxidative coupling of acetylene.^{27–31}

In searching for a new monomer class, initial Density Functional Theory (DFT) calculations (B3LYP, 6–311++G(d,p)) were performed to determine the acceptable electronic properties of potential monomers. Electron density maps were obtained for each of the monomers; an example is shown in Figure 1. The resultant polarization of the vinyl group was estimated by determining the charge on the internal and terminal carbons as well as the vinyl bond length by DFT calculations, then calculating the electric dipole moment along the double bond. Choosing a series of monomers that had been identified as either forming alternating

Author Manuscript

copolymers or incorporating, it was found that O-vinyl N-ethyl carbamate, a simple model monomer, had a similar electric dipole moment to those of vinyl acetate and vinyl t-butyl carbonate, both of which are known to form alternating copolymers (Figure 1c).^{20–23,26} By contrast, common monomers such as methyl methacrylate have dipole moments of opposite sign and do not form perfectly alternating copolymers.^{32,33}

Author Manuscript

Based on these initial studies, a series of O-vinyl carbamate monomers were prepared to test the functional group tolerance of the polymerization (Scheme 1). The monomers were prepared easily by reacting an appropriate free amine, vinyl chloroformate, and triethylamine in dry dichloromethane 19 h, followed by aqueous workup. For bifunctional monomers, the strong nucleophilicity of the amine allowed straightforward synthesis of other monomers containing unprotected functional groups such as -COOH (β -alanine) and -OH (2-hydroxybutylamine); such monomers were also purified by liquid-liquid extraction. The purity of the monomers was confirmed by ¹H and ¹³C NMR spectroscopy. The appearance of peak around 7.5 to 8 ppm in the ¹H NMR spectrum of the monomers corresponded to the -OCONH- group, confirming the carbamate linkage (Figures S1–S6).

Author Manuscript

Next, each of the synthesized monomers was copolymerized with sulfur dioxide at about -70°C with t-butylhydroperoxide as the initiator, followed by precipitation regardless of side chain structure (Scheme 1 and Figure S7). Analysis by ¹H NMR spectroscopy and GPC revealed that the polymers were free of unreacted monomer and possessed typical M_n of ~100 kDa, albeit with high molecular weight dispersity (Table S1). True alternation was also observed by ¹H NMR spectroscopy, which showed large peaks corresponding to -SO₂-CH₂-CHR-(6.4 and 4.0 ppm, respectively), but not those associated with homopolymerization of O-vinyl carbamates. The true alternation was also confirmed by integrating the peak at 6.4 ppm corresponding to -SO₂-CHR-CH₂- and comparing it to the peak at around 8 ppm corresponding to the side chain -OCONH- carbamate group. The integration matched perfectly in a 1:1 ratio. Moreover, analysis of NMR spectra showed that the R-group peaks were clearly preserved during the polymerization process, albeit with some expected broadening (Figures S1–S6). For example, expected peaks were maintained for R-groups after polymerization of carboxyls (1b to 2b, CH₂COOH, δ 3.2 ppm, Figure S2), esters (1c to 2c, -C(O)OCH₂-, δ 4.1 ppm, Figure S3), and azides (1e to 2e, -CH₂N₃, δ 3.4 ppm, Figure S5). Finally, primarily due to the high incorporation of SO₂ into the backbone, the polymers were generally soluble in DMSO, DMF, and dioxane; they were insoluble in more nonpolar solvents as well as protic solvents.

Author Manuscript

Initial proof-of-concept drug delivery studies focused on the incorporation of model drugs into polymer nanoparticles via nanoprecipitation. First, copolymer 2e was dissolved in DMSO along with the fluorophore Rhodamine B as a model drug and mixed for 30 min. The DMSO solution was then added drop-by-drop with stirring to PBS at pH 3 to create a turbid suspension. Nanoparticle Tracking Analysis showed that the particles were in a suitable size range for delivery,³⁴ with an average diameter of 185 nm and a standard deviation of 95 nm (Figure 2). The particles also had a visible pink color, confirming the encapsulation of Rhodamine B.

Next, the particle stability was determined as a function of pH. Suspensions of the nanoprecipitated particles were incubated in buffered saline at different pHs. At specific timepoints the particles were centrifuged down and the supernatant was removed for UV-Vis analysis, followed by replacement with the original buffer (Figure 2b). For the range of pH 1–5, the release was slow, with only 16 % released after 6 h. In the same timeframe at pH 7, release was shown to occur over 90% regardless of buffer salt. Based on ^1H NMR spectroscopy, the mechanism of degradation appeared to be an elimination reaction based on regeneration of the original monomer by a sulfone elimination mechanism (Figure S8).^{24,35} In our previous report, we showed that the poly(olefin-sulfone) was broken down into monomers by biologically relevant reactive oxygen species.²⁶ To check the potential of these particles as scaffolds for mucosal drug delivery, the stability of the Rhodamine B encapsulated particles in presence of potassium superoxide (KO_2) was determined. The particles were dispersed in MBS buffer (pH 5) and different amounts of KO_2 were added. At definite time intervals, it was centrifuged to collect the supernatant to analyze the release of dye followed by replacing original KO_2 solution. It was found that the particles were sensitive to 100 μM KO_2 (Figure 2d, S8).

While systemic nanoparticle delivery requires stability at neutral pH but release at acidic pH, mucus membranes have pH gradients that range from acidic at the exterior to neutral where the mucus contacts the lumen. As a proof-of-concept for simulating mucosal drug delivery mechanisms, release of contents from the particles was tested in a mucus model at different pH's. Acidity gradients are found within mucus such as gastric (pH 2 to 7) and vaginal (pH 4 to 7). An ideal particle will become entrapped in the mucus, then release its contents.

In order to simulate this process and show content release, the diffusivity of fluorescent cargo entrapped within the particles was determined as a function of pH. Briefly, simulated gastric mucus was formulated with mucin, polyacrylic acid, bovine serum albumin, DOPC, and cholesterol and allowed to sit at 4°C, followed by adjustment to the appropriate pH via addition of aqueous NaOH. Particles were prepared as above but with Alexa Fluor 488 (AF488) as the encapsulant, as the cationic Rhodamine B was found to associate with the highly carboxylated mucus matrix. Next, either AF488-loaded particles or free AF488 was added, and the mixture was allowed to sit for specific lengths of time. At each specific timepoint the diffusivity of the fluorescence in the particle-mucus formulation was measured by fluorescence recovery after photobleaching (FRAP) measurements using a confocal microscope (Figure 3). At pH 4 and 5, the diffusivity of both the particles and free dye at RT were different by an order of magnitude, with values of 40 and 2.8 $\mu\text{m}^2/\text{sec}$ at pH 4 and 86 and 7.5 $\mu\text{m}^2/\text{sec}$ at pH 5, respectively. The change in diffusivity for the mucus mimic from pH 4–5 is due to the presence of highly-carboxylated mucin and poly(acrylic acid) present in the mixture. At pH 8 after only 1.3 h incubation at 4°C, similar differences in magnitude were observed. However, after incubating 13 h at 4°C, the calculated diffusivity was similar to that of free dye, indicating dye release; this latter observation is most evident when scaling the diffusivity of AF488 with particles as compared to free AF488 (Figure 3c). Although 4°C is not specifically physiologically relevant, we were confined to this temperature to maintain fidelity of the mucus over this time scale.^{36,37} Finally, particles that had been incubated for over one week in mucus at pH 8 showed essentially the same diffusivity as free dye. These results are consistent with the dye release studies shown

previously within the cuvette for pH dependent release in solution, adjusting for the decrease in temperature from 25°C to 4°C. At the same time, the polymer particles were found to be essentially non-toxic to cells up to 200 µg/mL for 24 h incubation and up to 100 µg/mL for 48 h incubation. However, incubation times of 48 h are not common for mucus membranes; for example, the residence time of particle in vaginal mucus is estimated to be on the order of less than 4 h.^{38–40}

In conclusion, novel copolymers are reported in which alternating incorporation of sulfur dioxide results in an elimination depolymerization mechanism. DFT calculations of the dipole moment of the vinyl group were employed to find an acceptable range of electron donation was found such that the resulting copolymers were truly alternating. Based on this calculation, O-vinyl carbamates were synthesized with a variety of endgroups including carboxylic acids, alcohols, esters, and azides. These polymers were found to form perfectly alternating copolymers with sulfur dioxide. The polymers were then formulated into nanoparticles capable of encapsulating both Rhodamine B and Alexa Fluor 488, and the resulting particles were labile at pH > 6. Since the pH degradation profile was more suited for mucosal delivery than systemic delivery, the release of dye in a mucus-mimicking environment was validated using FRAP. Current efforts are focused on adapting the polymer particles for optimized drug delivery through mucosal barriers.

Supplementary Material

Refer to Web version on PubMed Central for supplementary material.

Acknowledgments

Funding Sources

This work was supported by NIH grants DP2EB020401 and R21EB020911. The authors thank Prof. Jennifer Cha for helpful discussions and Dr. Joseph Dragavon of the CU Biofrontiers Advanced Microscopy Core for help with FRAP experiments. Laser scanning confocal microscopy for FRAP imaging was performed on a Nikon A1R microscope acquired by the generous support of the NIST-CU Cooperative Agreement award number 70NANB15H226.

REFERENCES

1. Heller J, Barr J, Ng SY, Abdellauoi KS, Gurny R. *Adv. Drug Delivery Rev.* 2002; 54:1015.
2. Heffernan MJ, Murthy N. *Ann. Biomed. Eng.* 2009; 37:1993. [PubMed: 19513846]
3. Chien MP, Carlini AS, Hu DH, Barback CV, Rush AM, Hall DJ, Orr G, Gianneschi NC. *J. Am. Chem. Soc.* 2013; 135:18710–18713. [PubMed: 24308273]
4. Mynar JL, Goodwin AP, Cohen JA, Ma Y, Fleming GR, Fréchet JMJ. *Chem. Commun.* 2007:2081.
5. Goodwin AP, Mynar JL, Ma YZ, Fleming GR, Fréchet JMJ. *J. Am. Chem. Soc.* 2005; 127:9952. [PubMed: 16011330]
6. Wong AD, DeWit MA, Gillies ER. *Adv. Drug Delivery Rev.* 2012; 64:1031.
7. Sagi A, Weinstain R, Karton N, Shabat D. *J. Am. Chem. Soc.* 2008; 130:5434. [PubMed: 18376834]
8. Liu GH, Zhang GF, Hu JMI, Wang WR, Zhu MQ, Liu SY. *J. Am. Chem. Soc.* 2015; 137:11645. [PubMed: 26327337]
9. Zhang YF, Yin Q, Yin LC, Ma L, Tang L, Cheng JJ. *Angew. Chem. Int. Ed.* 2013; 52:6435.
10. Reineke TM. *ACS Macro Lett.* 2016; 5:14–18.
11. Olejniczak J, Chan M, Almutairi A. *Macromolecules.* 2015; 48:3166.

12. Li J, Rothstein SN, Little SR, Edenborn HM, Meyer TY. *J. Am. Chem. Soc.* 2012; 134:16352. [PubMed: 22950719]
13. Lux CD, Almutairi A. *ACS Macro Lett.* 2013; 2:432. [PubMed: 23814697]
14. Dewit MA, Gillies ER. *J. Am. Chem. Soc.* 2009; 131:18327. [PubMed: 19950931]
15. Chen EKY, McBride RA, Gillies ER. *Macromolecules.* 2012; 45:7364.
16. Paramonov SE, Bachelder EM, Beaudette TT, Standley SM, Lee CC, Dashe J, Fréchet JM. *Bioconjug. Chem.* 2008; 19:911. [PubMed: 18373356]
17. Murthy N, Thng YX, Schuck S, Xu MC, Frechet JM. *J. Am. Chem. Soc.* 2002; 124:12398. [PubMed: 12381166]
18. Seo W, Phillips ST. *J. Am. Chem. Soc.* 2010; 132:9234. [PubMed: 20565108]
19. DiLauro AM, Zhang H, Baker MS, Wong F, Sen A, Phillips ST. *Macromolecules.* 2013; 46:7257.
20. Jiang Y, Fréchet JM. *Macromolecules.* 1991; 24:3528.
21. Lee OP, Hernandez HL, Moore JS. *ACS Macro Letters.* 2015; 4:665.
22. Lobez JM, Swager TM. *Angew. Chem. Int. Ed.* 2010; 49:95.
23. Lobez JM, Swager TM. *Macromolecules.* 2010; 43:10422.
24. Sasaki T, Yaguchi H. *J. Polym. Sci. Polym. Chem.* 2009; 47:602.
25. Sasaki T, Yoneyama T, Hashimoto S, Takemura S, Naka Y. *J. Polym. Sci. Polym. Chem.* 2013; 51:3873.
26. Kumar K, Goodwin AP. *ACS Macro Lett.* 2015; 4:907.
27. Yang D, Ding SX, Huang JH, Zhao K. *Chem. Commun.* 2013; 49:1211.
28. Wakabayashi T, Ishii Y, Murata T, Mizobe Y, Hidai M. *Tetrahedron Lett.* 1995; 36:5585.
29. Nakagawa H, Okimoto Y, Sakaguchi S, Ishii Y. *Tetrahedron Lett.* 2003; 44:103.
30. Goossen LJ, Paetzold J, Koley D. *Chem. Commun.* 2003; 706
31. Foster DJ, Tobler E. *J. Am. Chem. Soc.* 1961; 83:851.
32. Matsuda M, Ishioroshi Y, Seki K. *J. Polym. Sci. Polym. Chem.* 1976; 14:1337.
33. Cais RE, Odonnell JH, Bovey FA. *Macromolecules.* 1977; 10:254.
34. Albanese A, Tang PS, Chan WCW. *Ann. Rev. Biomed. Eng.* 2012; 14:1. [PubMed: 22524388]
35. Yaguchi H, Sasaki T. *Macromolecules.* 2007; 40:9332.
36. Boegh M, Baldursdottir SG, Nielsen MH, Mullertz A, Nielsen HM. *Ann. Trans. of the Nor. Rh. Soc.* 2013; 21:233–240.
37. Dawson M, Krauland E, Wirtz D, Hanes J. *Biotechnol. Prog.* 2004; 20:851–8573. [PubMed: 15176891]
38. das Neves J, Bahia MF. *Int. J. Pharm.* 2006; 1:1.
39. Ensign LM, Hoen TE, Maisel K, Cone RA, Hanes JS. *Biomaterials.* 2013; 34:6922. [PubMed: 23769419]
40. Lai SK, Wang YY, Hanes JS. *Adv. Drug Delivery Rev.* 2009; 61:158.

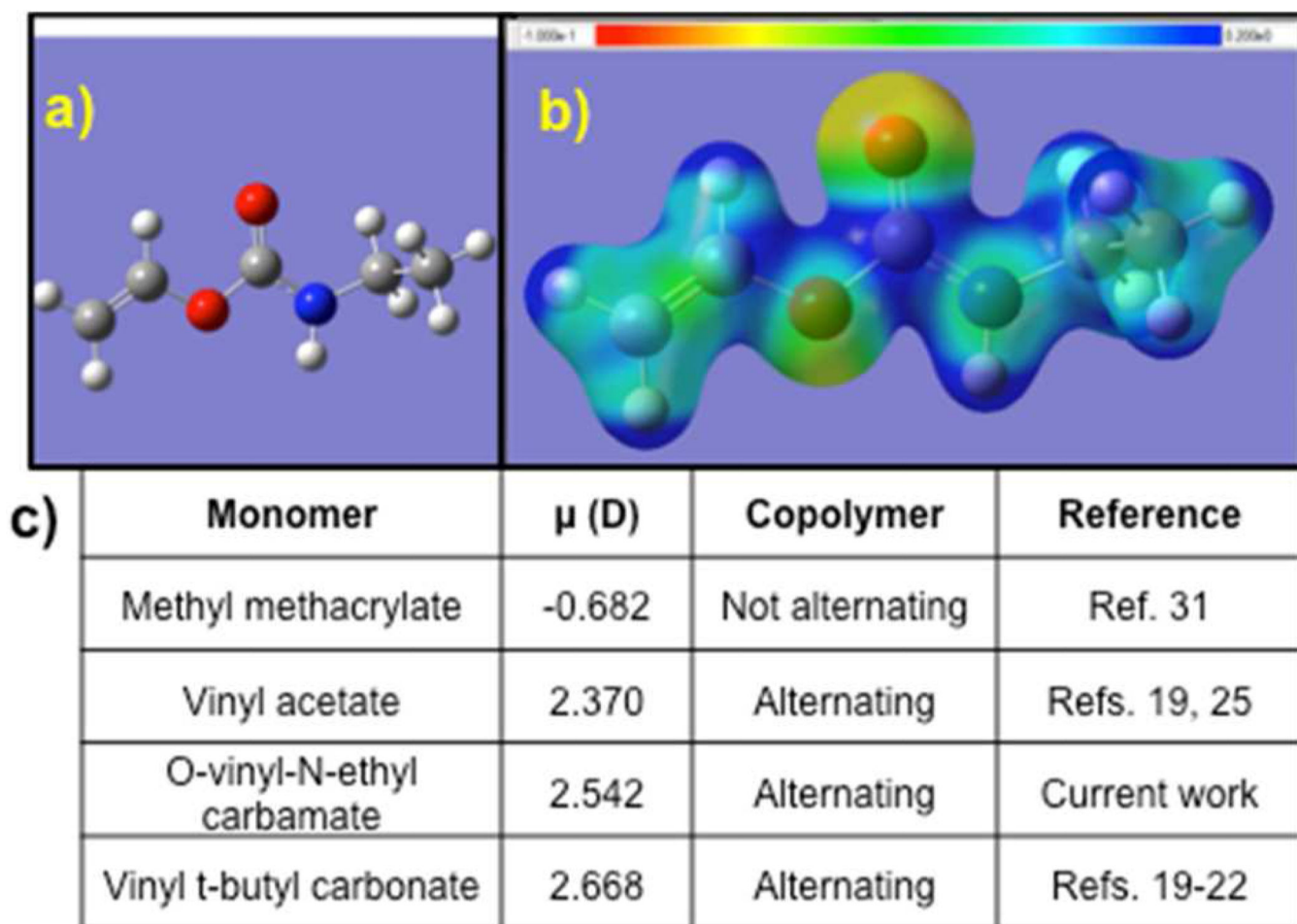


Figure 1. Properties and synthesis of O-vinyl N-ethyl carbamate monomers. a) Equilibrium geometry and b) electron density map of O-vinyl N-ethyl carbamate monomer. c) Dipole moment across vinyl group of select monomers, where + indicates donation into the vinyl group.

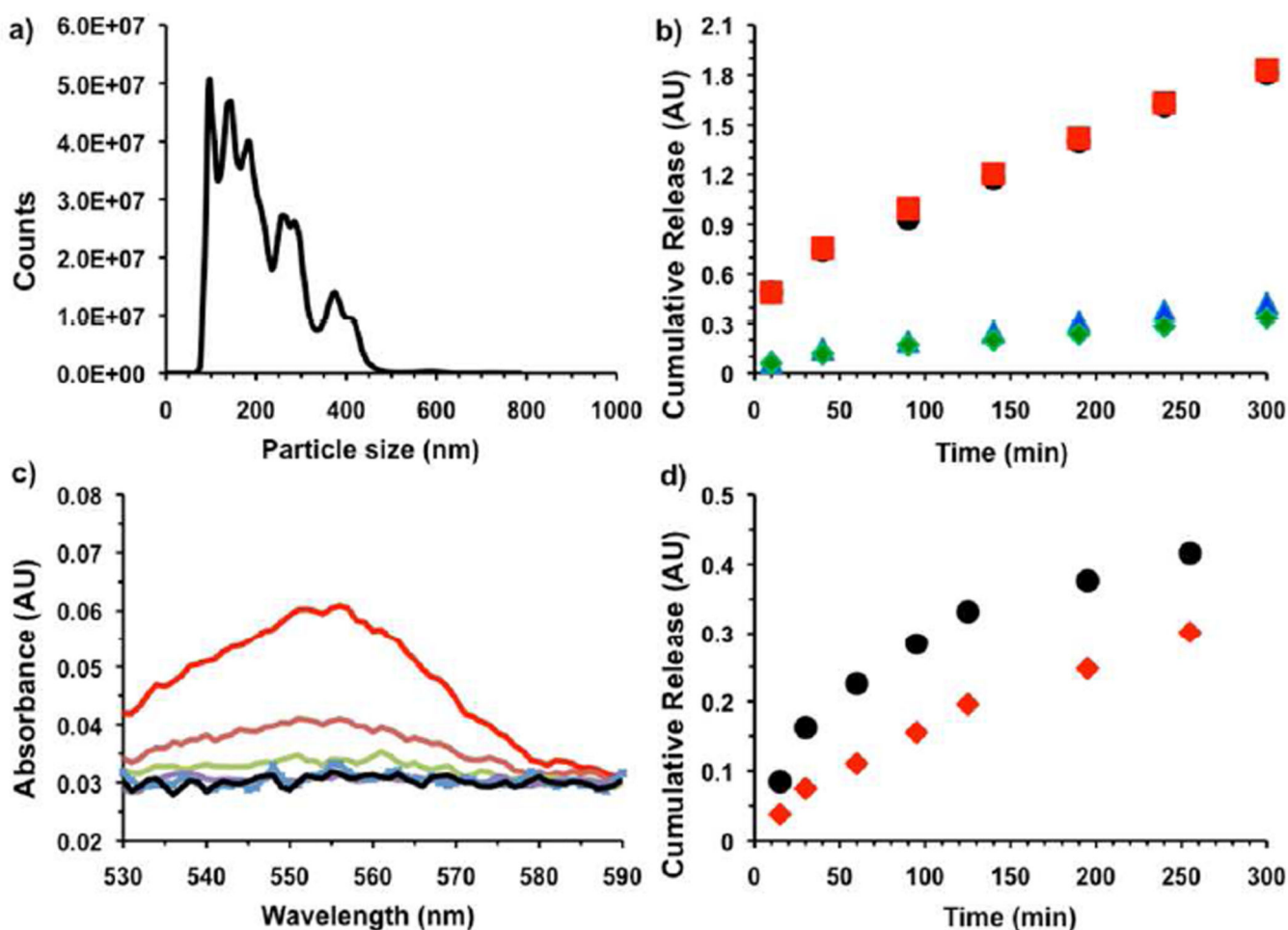


Figure 2.

a) Size histogram of Rhodamine B encapsulated nanoparticles as measured by Nanoparticle Tracking Analysis. b) Cumulative release of Rhodamine B from encapsulated nanoparticles with time at different pH. (black-pH 7.4 PBS), (red-pH 7.0 MBS), (blue-pH 5.3, MBS) and (green-pH 1.7 PBS). c) Release of Rhodamine B from encapsulated nanoparticles in presence of KO_2 after 20 min incubation time. (black- No KO_2), (red- 1×10^{-2} M KO_2), (brown- 1×10^{-3} M KO_2), (light green- 1×10^{-4} M KO_2), (violet- 1×10^{-5} M KO_2) and (light blue- 1×10^{-6} M KO_2), in pH 5 (MBS buffer). d) Cumulative release of Rhodamine B from encapsulated nanoparticles with time in presence of KO_2 (black- 1×10^{-3} M KO_2), (red- 1×10^{-4} M KO_2) in pH 5 (MBS buffer).

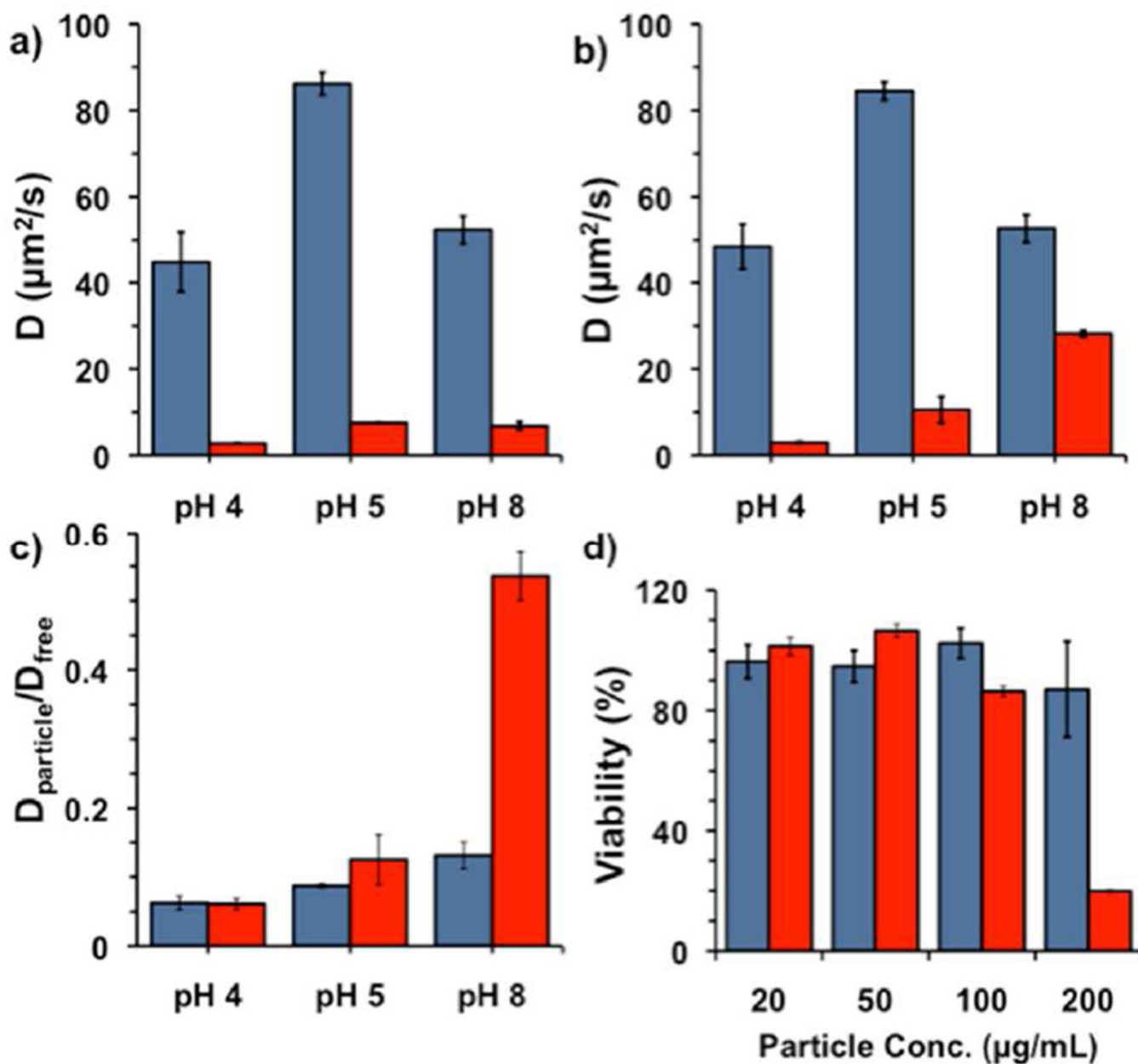
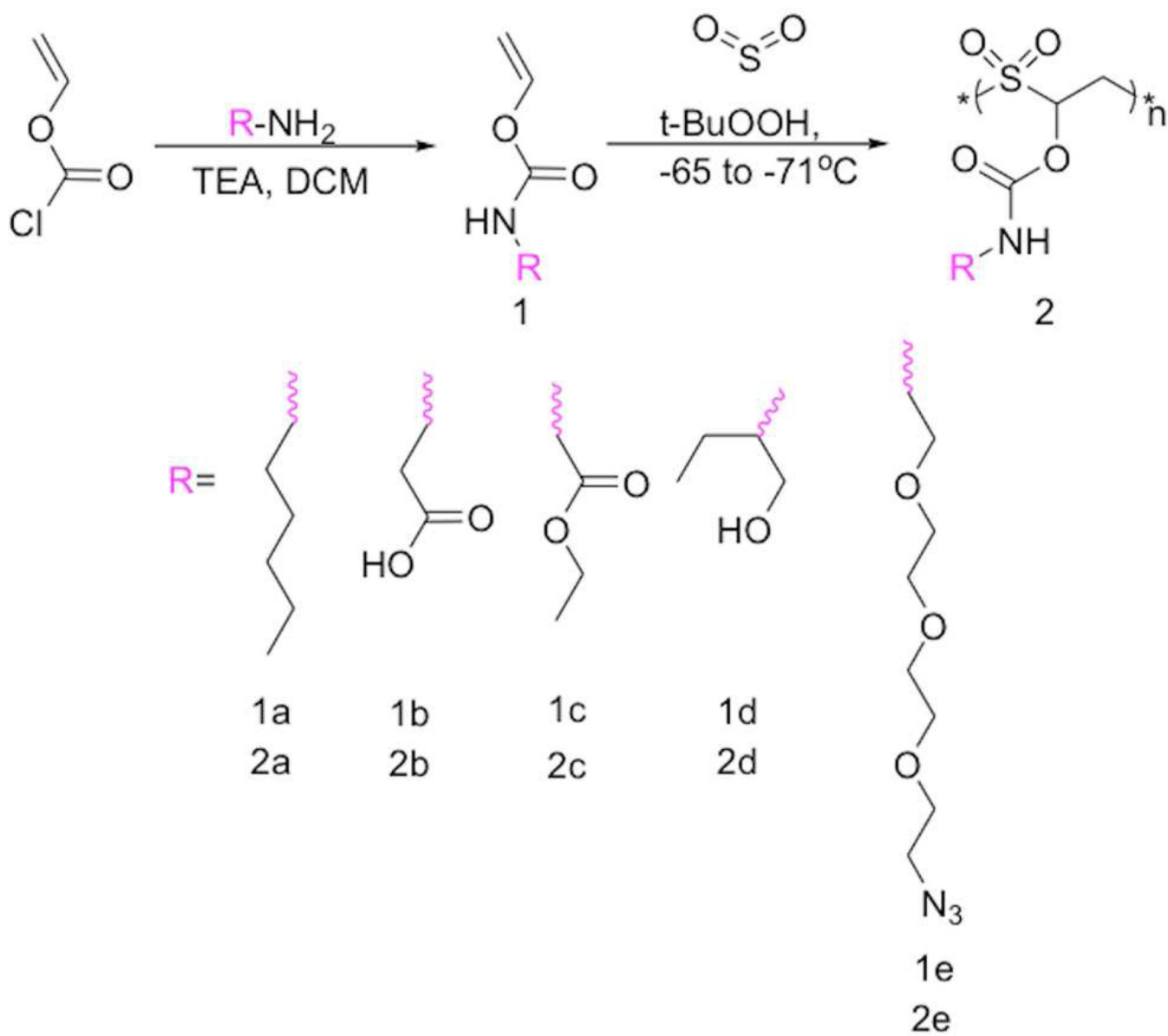


Figure 3. Diffusion coefficient calculated by fluorescence recovery after photobleaching (FRAP) for the free AF488 (blue) and AF488-loaded polymeric nanoparticles (red) in simulated mucus at different pH's. a) After incubation for 1.3 h at RT; b) after incubation for 13 h at 4°C. (c) Relative diffusivity of AF488 with particles vs. free AF488 for 1.3 h (blue) and 13 h (red). d) Viability of MDA-MB-231 cells after 24 (blue) and 48 h (red) incubation with indicated concentration of polymer particles.

**Scheme 1.**

General synthesis of O-vinyl carbamate monomers and poly(vinyl carbamate-*alt*-sulfur dioxide) polymers.